Molecular Biology of the Cell
Vol. 17, 3494–3507, August 2006

The Hsp90 Chaperone Complex Regulates GDI-dependent Rab Recycling

Christine Y. Chen* and William E. Balch*†‡

Departments of *Cell Biology and †Molecular Biology and ‡The Institute for Childhood and Neglected Disease, The Scripps Research Institute, La Jolla, CA 92037

Submitted December 2, 2005; Revised March 27, 2006; Accepted April 27, 2006
Monitoring Editor: Vivek Malhotra

Rab GTPase regulated hubs provide a framework for an integrated coding system, the membrome network, that controls the dynamics of the specialized exocytic and endocytic membrane architectures found in eukaryotic cells. Herein, we report that Rab recycling in the early exocytic pathways involves the heat-shock protein (Hsp)90 chaperone system. We find that Hsp90 forms a complex with guanine nucleotide dissociation inhibitor (GDI) to direct recycling of the client substrate Rab1 required for endoplasmic reticulum (ER)-to-Golgi transport. ER-to-Golgi traffic is inhibited by the Hsp90-specific inhibitors geldanamycin (GA), 17-(dimethylaminoethylamino)-17-demethoxygeldanamycin (17-DMAG), and radicicol. Hsp90 activity is required to form a functional GDI complex to retrieve Rab1 from the membrane. Moreover, we find that Hsp90 is essential for Rab1-dependent Golgi assembly. The observation that the highly divergent Rab GTPases Rab1 involved in ER-to-Golgi transport and Rab3A involved in synaptic vesicle fusion require Hsp90 for retrieval from membranes lead us to now propose that the Hsp90 chaperone system may function as a general regulator for Rab GTPase recycling in exocytic and endocytic trafficking pathways involved in cell signaling and proliferation.

INTRODUCTION

Rab proteins comprise a large family in the Ras superfamily of GTPases and play a crucial role in membrane trafficking in eukaryotic cells (Pfeffer and Aivazian, 2004). To date, >70 members of the Rab GTPase family have been identified (Pereira-Leal and Seabra, 2001). Each Rab is now thought to regulate specific steps in the complex exocytic and endocytic trafficking pathways that are a hallmark of eukaryotic cells. By alternating between the GTP (active) and GDP (inactive) states, Rab GTPases function as regulators of specialized hubs that control the assembly and disassembly of membrane tethering, targeting and fusion complexes that comprise the membrome network of eukaryotic cells (Gurkan *et al*., 2005).

Most Rab proteins are doubly prenylated by geranylgeranyl lipids at cysteine residues found at the C terminus (Khosravi-Far *et al*., 1991; Pereira-Leal *et al*., 2001). Prenylation is essential for membrane anchoring and Rab function (An *et al*., 2003; Calero *et al*., 2003; Gomes *et al*., 2003; Rak *et al*., 2003). Rab GTPases undergo membrane association and activation through the activity of Rab-specific guanine nucleotide exchange factors. After function and inactivation by GTPase-activating proteins (GAPs), guanine nucleotide dissociation inhibitor (GDI) retrieves Rab in the GDP-bound form from the membrane to the cytosol. GDI was first identified as a stabilizing factor for prenylated Rab3A in brain cytosol (Nishimura *et al*., 1995; Sasaki and Takai, 1995). To date, there are three mammalian isoforms of GDI (Alory and Balch, 2003). αGDI is highly enriched in brain tissue with low abundance in other cells, whereas δGDI is expressed specifically in muscle and adipocyte cells (Shisheva *et al*., 1994). βGDI is expressed ubiquitously in all cell types and is thought to be the "housekeeping" form of GDI (Nishimura *et al*., 1994; Bachner *et al*., 1995; Gurkan *et al*., 2005). GDI isoforms preferentially bind with high affinity to lipid modified Rabs in their GDP-bound form (Sasaki and Takai, 1995; Rak *et al*., 2003). Despite their different tissue expression patterns, most GDI isoforms have been demonstrated to recognize a broad range of Rab species in vitro. In vivo, differentially expressed GDI isoforms are likely specialized for abundant recycling pathways such as that found for αGDI in recycling of Rab3A involved in neurotransmitter release at synapses in the brain (Sudhof, 2004). Thus, unlike other Rab effectors such as guanine nucleotide exchange factors (GEFs) and GAPs that are specific for each Rab family member (Pfeffer and Aivazian, 2004), GDI serves as a generic regulator for recycling of Rab GTPases (Alory and Balch, 2003) for use in multiple rounds of membrane transport.

The structure of αGDI has been solved by x-ray crystallography (Schalk *et al*., 1996; An *et al*., 2003; Rak *et al*., 2003). GDI is a two domain protein with an upper domain I involved in binding the Rab effector domain, and a lower domain II helical tripod containing prenyl-lipid binding surfaces (Luan *et al*., 1999, 2000; Alory and Balch, 2003; An *et al*., 2003; Rak *et al*., 2003; Pylypenko *et al*., 2006). Intriguingly, in the Rab-free structure, the helical tripod is found in a tightly packed, closed configuration (Schalk *et al*., 1996; An *et al*., 2003); upon Rab binding, the domain II helical tripod opens to form a deep binding pocket for the prenyl lipids (Rak *et al*., 2003; Pylypenko *et al*., 2006). The mechanism by which this occurs remains to be defined.

The yeast *Saccharomyces cerevisiae* contains only one GDI, Gdi1p, that is essential for growth (Garrett *et al*., 1994). Genetic analysis of function in yeast revealed that Gdi1p association with membranes is independent of Rab and requires a specific region, referred to as mobile effector loop

This article was published online ahead of print in *MBC in Press* (http://www.molbiolcell.org/cgi/doi/10.1091/mbc.E05–12–1096) on May 10, 2006.

Address correspondence to: William E. Balch (webalch@scripps.edu).

(MEL), located at the interface of domains I and II (Luan *et al*., 1999; Luan *et al*., 2000; Alory and Balch, 2003), raising the possibility that additional factors facilitate GDI recruitment to the bilayer for Rab retrieval from membranes. Consistent with this, we have demonstrated that the brain-specific αGDI isoform uses a membrane-associated heat-shock protein (Hsp)90 chaperone complex to retrieve Rab3A from synaptic vesicle membranes found at the synapse (Sakisaka *et al*., 2002). Physiologically, Hsp90-dependent retrieval of Rab3A is critical for Ca^{2+}-induced neurotransmitter release (Sakisaka *et al*., 2002), suggesting that failure of αGDI to retrieve Rab3A prevents sequential maturation events involved in synaptic vesicle targeting and fusion.

Hsp90 is the core component of an abundant and ubiquitous cytosolic chaperone machine that uses a variety of cochaperones to regulate the activity of different client proteins, including steroid hormone receptors and signaling kinases (Pratt and Toft, 2003; Pratt *et al*., 2004). Hsp90 has a unique ATP-binding site in its N-terminal domain that binds the well-characterized drugs geldanamycin (GA) and radicicol, and more recent clinically relevant analogs of GA, 17-desmethoxy-17-*N*,*N*-dimethylaminoethylamino-geldanamycin (17-DMAG) (Jez *et al*., 2003), or 17-allylaminogeldanamycin (17-AAG) (Pratt *et al*., 2004; Miyata, 2005). The binding of GA or radicicol to Hsp90 prevents activation by binding of ATP and therefore arrests the chaperone cycle, inhibiting client protein function or targeting client proteins for degradation (Prodromou *et al*., 1997; Panaretou *et al*., 1998). To date, >100 different GA/radicicola-sensitive Hsp90 client substrates have been identified (Pratt and Toft, 2003). All known Hsp90 chaperone–client interactions are inhibited by Hsp90-specific antagonists. One of the best characterized Hsp90 chaperone clients is the steroid hormone receptor (SHR) (Pratt *et al*., 2004). Here, the chaperone activity of the Hsp90 complex is used to dynamically regulate the conformation of SHR to transiently open a deep hydrophobic pocket accessible from the protein surface for binding of its steroid ligand (Pratt and Toft, 1997, 2003). The striking conformational change observed in the domain II helical tripod of GDI from a closed to open configuration to accommodate the prenyl group during membrane retrieval (Schalk *et al*., 1996; Rak *et al*., 2003; Pylypenko *et al*., 2006) is highly reminiscent of the mechanism by which SHR uses Hsp90 to transiently generate a binding pocket for hormone binding.

The role of Hsp90 in Rab3A recycling could reflect the highly regulated process of neurotransmitter release (Sakisaka *et al*., 2002). To address whether Hsp90 activity is required for other Rab-dependent steps, we have now focused on the well characterized Rab1-dependent endoplasmic reticulum (ER) to Golgi constitutive transport pathway (Plutner *et al*., 1991; Nuoffer *et al*., 1994; Peter *et al*., 1994; Pind *et al*., 1994; Wilson *et al*., 1994; Allan *et al*., 2000). Dominant negative Rab1 mutants potently inhibit ER-to-Golgi cargo trafficking in mammalian cells (Plutner *et al*., 1991; Nuoffer *et al*., 1994). Moreover, interfering with Rab1 function destabilizes the Golgi stack, leading to fragmentation and loss of function (Wilson *et al*., 1994). We have recently shown that after treatment of cells with brefeldin A (BFA), a drug that triggers collapse of the Golgi to the ER, Rab1 is required for Golgi reassembly (Bannykh *et al*., 2005). In contrast to Rab3A, which regulates the highly specialized targeting-fusion hub controlling release of neurotransmitter release from synaptic vesicles in the neuron (Sudhof, 2004; Gurkan *et al*., 2005), Rab1 is ubiquitously expressed in all cell types and has a conserved function in regulating targeting-fusion hubs that control ER-to-Golgi transport in both lower and higher eukaryotes (Pereira-Leal *et al*., 2001; Pereira-Leal and Seabra, 2001; Gurkan *et al*., 2005). Using GA and radicicol to examine the potential role of Hsp90 in Rab1 function, we find that GDI-dependent retrieval of Rab1 from the Golgi membranes in vitro, and ER-to-Golgi transport and Golgi assembly in vivo, require Hsp90 chaperone complex function. These results have important implications for understanding the global mechanism of Rab recycling in membrane trafficking pathways and provides insight into the potential effects of Hsp90 as a chemotherapeutic target for inhibition of cell proliferation in metastatic disease using GA analogs (Cheng *et al*., 2005; Miyata, 2005; Pearl, 2005).

MATERIALS AND METHODS

Materials

GA and radicicol were purchased from Sigma-Aldrich (St. Louis, MO). 17-DMAG and 17-AAG were generous gifts provided by Dr. D. Santi (Kosan, San Francisco, CA). All other chemicals were purchased from Sigma-Aldrich unless otherwise indicated. Protein G beads were purchased from GE Healthcare (Piscataway, NJ), cell culture medium was purchased from Invitrogen (Carlsbad, CA), fetal bovine serum (FBS) was purchased from Gemini (Woodland, CA), and bovine growth serum was purchased from Hyclone Laboratories (Logan, UT). Easy-tag [^{35}S]methionine (Met) and [α^{32}P]ATP were purchased from PerkinElmer Life and Analytical Sciences (Boston, MA). A monoclonal antibody (mAb) against αGDI (cl81.2) was a kind gift from Dr. R. Jahn (The Max-Plank Institute for Biophysical Chemistry, Göttingen, Germany), polyclonal antibody against αGDI (p609) was generated by injecting rabbit with recombinant bovine GDI using standard procedures, polyclonal antibody against α1-anti-trypsin was purchased from MP Biomedicals (Irvine, CA), polyclonal antibody against transferrin was provided by S. Schmid (TSRI, La Jolla, CA), polyclonal antibody against albumin was purchased from Sigma-Aldrich, polyclonal antibody against Rab1(p8868) was generated as described previously (Plutner *et al*., 1991), monoclonal (SPA 830) and polyclonal antibody (SPA 846) against Hsp90 were purchased from Stressgen (San Diego, CA), mAb (3G3) to immunoprecipitate Hsp90 was purchased from Abcam (Cambridge, MA); polyclonal Man II antibody was obtained from M. Farquhar (University of California, San Diego, San Diego, CA), monoclonal GM130 antibody was purchased from BD Transduction Laboratories (San Jose, CA); polyclonal antibody against vesicular stomatitis virus (VSV)-G^{ts} was generated as described previously (Rowe *et al*., 1996), and monoclonal (P5D4) antibody was generated by hybridoma cells from American Type Culture Collection (Manassas, VA).

Cell Culture

Normal rat kidney (NRK) and HepG2 cells were maintained in DMEM medium supplemented with 5% bovine growth serum or 10% FBS, respectively. Chinese hamster ovary (CHO)-K1 cells were maintained in α-minimal essential medium supplemented with 7.5% FBS. All cells were incubated at 37°C in a 5% CO_2 atmosphere.

In Vivo Transport Assays

The tsO45 strain of VSV (VSV^{ts}) was used to infect NRK cells as described previously (Plutner *et al*., 1992). In brief, NRK cells were grown until 90% confluent and infected with 10 plaque-forming units/cell of virus at 32°C for 45 min in serum-free medium and incubated in growth medium at 32°C for 3.5 h. For pulse-chase experiments, cells were transferred to a 40°C water bath, rinsed three times with Met-free medium, pulse-labeled with 100 μCi of [^{35}S]Met for 10 min, and then chased for 2 min. All Hsp90 inhibitors were added after the chase period at 40°C for indicated amount of time as described in *Results*. After drug treatment, cells were washed three times with phosphate-buffered saline (PBS) and then treated with 0.25% trypsin for 1 min on ice followed by 1 ml of DMEM with 2 mg/ml trypsin inhibitor to neutralize trypsin. Trypsinized cells were removed from the dish and transferred to Eppendorf tubes. After incubation at 32°C, cells were pelleted at 16,000 × *g* for 1 min at 4°C, lysed (50 mM Tris-Cl, pH 7.5, 100 mM NaCl, 1 mM EDTA, 1% Triton X-100, and 1 mM phenylmethylsulfonyl fluoride), and the lysate was centrifuged at 16,000 × *g* for 10 min and VSV-G^{ts} was immunoprecipitated with the mAb P5D4. Immunoprecipitated proteins were digested with endoglycosidase H (endo H) and analyzed by SDS-PAGE and autoradiography. All samples were quantitated using a PhosphoImager (Molecular Devices, Sunnyvale, CA) in the linear range.

To follow the transport of α-1 antitrypsin (α1-AT), transferrin, and albumin, 5×10^5 HepG2 cells were seeded in six-well dishes. Cells were incubated in Met-free medium for 1 h, and pulse-labeled with the indicated amount of drug for 30 min followed by 0, 15, and 30 min of chase. Medium was collected, and cells were lysed with lysis buffer (60 mM Tris-HCl, pH 7.4, 190 mM NaCl, 6 mM EDTA, 0.4% SDS, and 2% Triton X-100). The cell lysate was passed

Table 1. *S. cerevisiae* strains used in this study

Strain	Genotype	Reference
YPH 499	MAT**a** *ura 3-52 lys2-801^{amber} ade2-101^{orchre} trp1-Δ 63 his3-Δ 200 leu 2-Δ 1*	Kimura *et al.* (1994)
G170D (YOK5)	MAT**a** *ura 3-52 lys2-801^{amber} ade2-101^{orchre} trp1-Δ 63 his3-Δ 200 leu 2-Δ 1, hsc82::URA3 hsp82-4::LEU2*	Kimura *et al.* (1994)
A97T (YOK25)	MAT**a** *ura 3-52 lys2-801^{amber} ade2-101^{orchre} trp1-Δ 63 his3-Δ 200 leu 2-Δ 1, hsc82::URA3 hsp82-38::LEU2*	Kimura *et al.* (1994)
T101I (YOK27)	MAT**a** *ura 3-52 lys2-801^{amber} ade2-101^{orchre} trp1-Δ 63 his3-Δ 200 leu 2-Δ 1, hsc82::URA3 hsp82-2::LEU2*	Kimura *et al.* (1994)

through a 27-gauge needle twice to shear DNA. Both the medium and the cell lysate were precleared by incubating with 5 μl of normal rabbit serum and 30 μl of protein G beads for 1 h at 4°C. After incubation, beads and cell debris were pelleted at 14,000 rpm for 10 min at 4°C, and the supernatant was collected for immunoprecipitation using 4 μl of anti-α1-AT goat antiserum, 4 μl of anti-transferrin sheep antiserum, or 5 μl of anti-albumin goat antiserum in the presence of 30 μl of protein G beads overnight at 4°C. After immunoprecipitation, beads were washed twice with buffer A (50 mM Tris-HCl, pH 7.5, 5 mM EDTA, 150 mM NaCl, 0.1% Triton X-100, and 0.02% SDS) and twice with buffer B (50 mM Tris-HCl, pH 7.5, 5 mM EDTA, and 150 mM NaCl). Immunoprecipitated proteins were digested with endo H and analyzed by SDS-PAGE and autoradiogragphy.

Table 1 lists the *S. cerevisiae* strains used in the present study. Parental wild-type strain YPH499 and *hsp82* mutants (G170D, A97T, and T101I; previously named YOK5, YOK25, and YOK27, respectively) were grown at 25°C in YPD-rich medium or standard minimal medium, supplemented as necessary (Sherman, 1986). To follow carboxypeptidase Y (CPY) transport, wild type and mutants were cultured in the presence of 40 μM radicicol or at the indicated temperature before analysis. Metabolic labeling and immunoprecipitation of CPY protein were performed as described previously (Klionsky, 1998). Immunoprecipitated CPY proteins were analyzed by SDS-PAGE followed by autoradiography.

Immunofluorescence

NRK cells were seeded on coverslips 1 d before infection. After infection with VSV^{ts}, cells were maintained in DMEM medium at 40°C for 2 h. GA, radicicola, or dimethyl sulfoxide (DMSO) vehicle was added to medium for an additional 30 min before shift to 32°C for the indicated time in *Results* and fixed with 4% formaldehyde in for 15 min at room temperature. Coverslips were washed four times with PBS, blocked in PBS containing 0.1% Triton X-100, 0.25% bovine serum albumin for 5 min, incubated with primary antibody for 1 h at room temperature, washed three times with PBS, and then incubated with secondary antibody coupled to Texas-Red or Oregon Green for 30 min at room temperature, washed three times with PBS, and mounted. Images were taken using a Bio-Rad confocal microscope (Bio-Rad 1024; Bio-Rad, Hercules, CA). To analyze the size distribution of Golgi, all images were taken at the same setting and images were recorded in an identical manner and quantitated using LaserSharp software (Bio-Rad) and the ImageJ program (National Institutes of Health, Bethesda, MD). Signal threshold and the determination of particle size were obtained using the default configuration. Images were pseudocolored by Photoshop 7 (Adobe Systems, San Jose, CA). To analyze the colocalization of GM130 and VSV-G^{ts}, the z-series images were collected from each marker and projected to a single image. The overlap between two markers was analyzed by the LaserSharp software. At least 10 cells were counted for measuring the colocalization.

Complementation Assay

All expression plasmids were generated using a pc3.1 vector (Invitrogen). Cells were transfected using Lipofectamine 2000 (Invitrogen) following the manufacturer instructions. CHO cells (4×10^5) were seeded overnight into six-well dishes before transfection. Transient expression was performed by transfection of CHO cells with empty vector (mock), Rab1B, Rab3A, or Sar1A as described in *Results*. Twenty-four hours after transfection, cells were infected with VSV^{ts} as described above. After 3.5 h postinfection, cells were rinsed with Met-free medium at 40°C and pulse-labeled with 25 μCi of [^{35}S]Met followed by 2-min chase. 20 μM GA or 40 μM radicicol was added to medium for 30 min before shifting to 32°C for additional 30 min. VSV-G^{ts} was recovered and immunoprecipitated as described above.

Immunoprecipitation of the Hsp90/GDI Complex

NRK cells harvested from a confluent 15-cm dish (~5×10^7 cells) were incubated with 20 μM GA or 0.1% DMSO in DMEM at 37°C for 4 h. Each dish was washed one time with 10 ml of PBS and incubated with 1 ml of trypsin/EDTA briefly at room temperature. Cells were removed from the dish with 5 ml of PBS and harvested by centrifugation at 1500 rpm for 10 min at 4°C, and then washed one time with 5 ml of 50 mM Tris-HCl, pH 7.5. The cell pellet was resuspended with 1 ml of lysis buffer (50 mM Tris-HCl, pH 7.5, 100 mM KCl, 5 mM $MgCl_2$, and 2 mM dithiothreitol) with protease inhibitor tablets (Roche Diagnostics, Indianapolis, IN) and homogenized with a ball-bearing homogenizer (Balch and Rothman, 1985). The homogenate was centrifuged at 60,000 rpm for 15 min, and the supernatant was incubated with 50 μl antibody conjugated to protein G beads at 4°C for 4 h. After binding, the resin was washed four times with 1 ml of lysis buffer at 4°C, and bound proteins were eluted by addition of 40 μl of 1× loading buffer (50 mM Tris-HCl, pH 6.8, 2% SDS, and 10% glycerol).

Electron Microscopy

NRK cells were plated in 35-mm dishes. After treatment as described in the *Results*, cells were fixed in 2.5% glutaraldehyde in 0.1 M cacodylate buffer. After a brief buffer wash, cells were postfixed in 1% osmium tetroxide, treated with 0.5% tannic acid-1% sodium sulfate, cleared in 2-hydroxypropyl methacrylate, and embedded in LX112 (Ladd Research, Williston, VT). Embedded cells were sectioned for electron microscopy and imaged on a Philips CM100 electron microscope (FEI, Hillsbrough OR).

RESULTS

GDI Is Associated with Hsp90

To determine whether GDI-dependent recycling of Rab1, like Rab3A (Sakisaka *et al*., 2002), reflects interaction with Hsp90 when recruited to the Golgi complex, a Golgi-enriched membrane fraction was prepared from NRK cells (Balch *et al*., 1984), solubilized in 0.5% CHAPS, and GDI-precipitated with GDI-specific mAb using protein G beads. As shown in Figure 1A, using immunoblotting to identify components that coimmunoprecipitate with GDI, we detected bands that cross-react with both Hsp90 and Rab1-specific antibodies. A similar result was observed using both Rab1- and Hsp90-specific antibodies. Quantitation of the immunoblots revealed that the pool of Hsp90 bound to the GDI complex is ~1% of total Hsp90 present in the enriched Golgi fraction, which may contain up to 15 different Rab GTPases (Gurkan *et al*., 2005) and other Hsp90-dependent signaling kinases. The amount of GDI recovered with Rab1- or Hsp90-specific antibodies was significantly lower than that observed with GDI-specific antibodies. This is consistent with the interpretation that Hsp90/GDI are likely complexed with different Rab GTPases. Thus, like αGDI in the synapse that is found transiently associated with an Hsp90 chaperone complex and Rab3A (Sakisaka *et al*., 2002), a membrane-associated form of GDI also may be transiently localized to the Golgi and associated with Rab1 through Hsp90.

We also examined the cytosolic pool to determine whether a soluble Hsp90–GDI–chaperone client complex can be detected. Using gel filtration chromatography, we observed two cytosolic pools of GDI. The first pool contained >90% of the total GDI. This pool eluted as an ~80-kDa complex that coeluted with Rab1, reflecting the abundant cytosolic pool containing GDI–Rab heterocomplexes (Figure 1B, top) (Soldati *et al*., 1993; Ullrich *et al*., 1993; Sanford *et al*., 1995). Interestingly, GDI also was detected in a minor (<10%) higher molecular weight pool that lacked Rab1 that had a molecular weight consistent with a protein complex of 300–400 kDa. Immunoprecipitation of GDI from this complex revealed the presence of coprecipitating Hsp90 (Figure 1B,

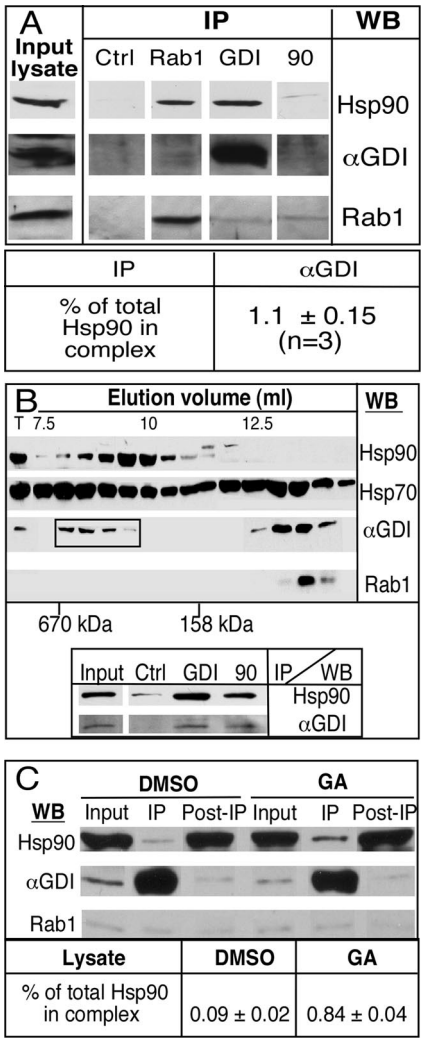

Figure 1. αGDI complexes in enriched Golgi fractions and cytosol. (A) An enriched Golgi fraction from NRK cells (Balch *et al*., 1984) was solubilized and incubated with antibody conjugated with P5D4 (control), c181.2(GDI), m5C6(Rab1), or 3G3(Hsp90) as described in *Materials and Methods*. Hsp90, αGDI, and Rab1 were detected using immunoblotting with specific antibody. Shown is 2% of input lysate and 50% of the αGDI immunoprecipitate. Typical result of duplicate experiments is shown. (B) αGDI exists in a high-molecular-weight complex in cytosol. Cytosol prepared from NRK cells was separated using size exclusion chromatography as described in *Materials and Methods*. Fractions were collected and analyzed by immunoblotting with the indicated antibody. Fractions between 8 and 10 ml were collected (indicated by boxed area) and subject to immunoprecipitation that shown in bottom panel. (C) A cytosolic GDI–Hsp90 complex is stabilized by GA. αGDI was immunoprecipitated from equal amounts of cytosol prepared from DMSO- or GA-treated cells. Shown is 1% of the input cytosol, 1% unbound fraction, and 50% of the αGDI immunoprecipitate. Typical result of duplicate experiments is shown.

bottom). A similar result was observed by precipitating with Hsp90. These results suggest that GDI and Hsp90 can form a higher molecular weight complex.

GA is a specific inhibitor of Hsp90 function. Incubation Hsp90 in the presence of GA results in accumulation of Hsp90 client proteins in chaperone cycle intermediates (Pratt *et al*., 2004). To determine whether GA would affect stability of this putative cytosolic intermediate, cells were preincubated with GA before lysis. In the presence of GA, the cytosolic

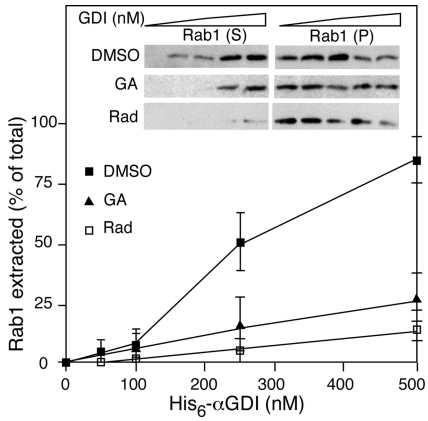

Figure 2. Hsp90 activity is required for extraction of Rab1 in vitro by αGDI. Extraction of Rab1 by increasing concentrations of recombinant αGDI from semi-intact NRK cells was performed as described previously (Peter *et al*., 1994). To test the effect of Hsp90 inhibitors, cells were pretreated with 20 μM GA or 50 μM radicicol (Rad) for 60 min before preparation of semi-intact cells. A typical experiment is shown in the inset. Quantitation based on the average of three independent experiments. Error bars indicate SEM.

associated Hsp90-GDI client complex increased by 10-fold, although a corresponding increase in Rab1 was not detected (Figure 1C). Therefore, as has been observed for other Hsp90–client complexes (Pratt and Toft, 2003), the GA-sensitive cytosolic pool may reflect a transient, substrate-free intermediate in the Rab1 recycling pathway.

Rab1 Retrieval from Membranes Requires Hsp90

To study the potential role of Hsp90 in Rab1 recycling by GDI, we examined biochemically the effect of the Hsp90 inhibitor GA and radicicol on GDI retrieval of Rab1 from Golgi membranes in vitro. We have previously demonstrated that semi-intact cells provide a robust in vitro model system to study GDI-dependent Rab1 retrieval and Rab1-dependent ER-to-Golgi transport (Beckers *et al*., 1989; Plutner *et al*., 1991, 1992; Pind *et al*., 1994; Allan *et al*., 2000). Semi-intact perforated NRK cells were prepared to expose the Rab1-containing Golgi compartments (Peter *et al*., 1994). When semi-intact cells were incubated with increasing concentrations of recombinant αGDI, membrane-bound Rab1 was efficiently extracted from the membranes to the soluble pool as observed previously (Peter *et al*., 1994) (Figure 2A). In contrast, when cells were treated with GA to inactivate the endogenous Hsp90 pool before perforation, the efficiency of Rab1 extraction by incubation of semi-intact cells with recombinant αGDI was reduced fourfold (Sakisaka *et al*., 2002) (Figure 2A). Preincubation with radicicol resulted in an eightfold reduction in Rab1 extraction (Figure 2A). These results suggest that like GDI-dependent Rab3A recycling at the synapse (Sakisaka *et al*., 2002), Rab1 retrieval from Golgi membranes found in the early secretory pathway is sensitive to an Hsp90-dependent step.

VSV-G^{ts} Transport between ER to Golgi Is Sensitive to Hsp90 Inhibitors

Given the observed interactions of GDI with Hsp90 and the sensitivity of GDI-dependent retrieval of Rab1 to GA, we examined the role of Hsp90 inhibitors on the transport of cargo from the ER to the Golgi. Given that GA and radicicol are known to bind to the ATP-binding site on the N-terminal domain of Hsp90 (Schulte *et al*., 1998), we were concerned

that GA and/or radicicol may inhibit the ubiquitous ATP-dependent chaperone *N*-ethylmaleimide sensitive factor (NSF) that mediates SNARE-dependent fusion reactions involved in ER-to-Golgi and intra-Golgi transport (Whiteheart *et al*., 1994) and p97, an ATPase involved in ER-to-Golgi and intra-Golgi in tethering events (Rabouille *et al*., 1995). In both cases, we measured the effects of the drugs on ATPase activity in vitro using purified recombinant protein (Figure 3A) (Whiteheart *et al*., 1994). Whereas the ATPase activity of NSF was sensitive to pretreatment with the alkylating agent *N*-ethylmaleimide as reported previously (Block *et al*., 1988), neither NSF nor p97 were sensitive to either of the Hsp90 inhibitors at concentrations that potently inhibit Hsp90. These results are consistent with the known high specificity of GA, its analogs, and radicicol for Hsp90–client chaperone pathways.

To follow transport of cargo, we used a temperature-sensitive variant (tsO45) of vesicular stomatitis virus glycoprotein (VSV-G^{ts}), a type I transmembrane membrane that acquires two high-mannose, *N*-linked glycans during translocation into the ER. NRK cells infected with VSV^{ts} at the restrictive temperature (40°C) retain the protein in the ER. After downshift to the permissive temperature (32°C), a synchronous wave of VSV-G^{ts} exits the ER in a COPII-dependent manner (Beckers *et al*., 1987; Rowe *et al*., 1996; Aridor *et al*., 1998). Transport to the Golgi can be followed morphologically using indirect immunofluorescence (Plutner *et al*., 1992) or biochemically as a consequence of sequential processing of VSV-G^{ts} *N*-linked glycans to complex structures in the *cis*-, *medial*-, and *trans*-Golgi compartments (Beckers *et al*., 1990). Golgi-processed forms, but not ER forms, of VSV-G^{ts} are resistant to digestion after incubation of detergent-solubilized cell lysates with endo H. A characteristic mobility shift observed using SDS-PAGE after endo H digestion allows us to distinguish the high mannose *N*-glycan structures in the ER that are endo H sensitive (Figure 3B, band S) from early processing intermediates in the *cis*/*medial*-Golgi compartments (Figure 3B, band I) and late *trans*-Golgi mature complex forms (Figure 3B, band R). Use of synchronized export of VSV-G^{ts} in combination with acquisition of endo H resistance provides a useful tool to assess the effects of membrane permeant small molecule inhibitors such as GA and radicicol on VSV-G^{ts} trafficking from the ER through Golgi compartments.

We first examined the effects of Hsp90 inhibitors on transport of VSV-G^{ts} from the ER to the Golgi in viral-infected cells using a pulse-chase protocol. Infected NRK cells expressing VSV-G^{ts} were labeled with [^{35}S]Met at the restrictive temperature. Hsp90 is a cytosolic chaperone that is known to be essential for folding of multimembrane spanning proteins, including the cystic fibrosis transmembrane regulator (CFTR) during translocation into the ER. Synthesis of CFTR in the presence of GA results in its degradation (Loo *et al*., 1998). We have observed a similar affect on the synthesis of VSV-G^{ts} (our unpublished data). To avoid direct effects of Hsp90 inhibitors on VSV-G^{ts} stability during synthesis, Hsp90 inhibitors were added to the medium after labeling with [^{35}S]Met. After the pulse, cells were incubated with the Hsp90 inhibitors GA, radicicol, 17-DMAG, and 17-AAG for 1 h at the restrictive temperature (40°C) (to retain VSV-G^{ts} in the ER) while exposing the abundant Hsp90 cytoplasmic pool to each of the drugs to promote inactivation before shift to 32°C to initiate transport. After 30-min incubation at 32°C, cells were transferred to ice, solubilized, and the fraction of VSV-G^{ts} processed to endo H-resistant forms was determined using SDS-PAGE.

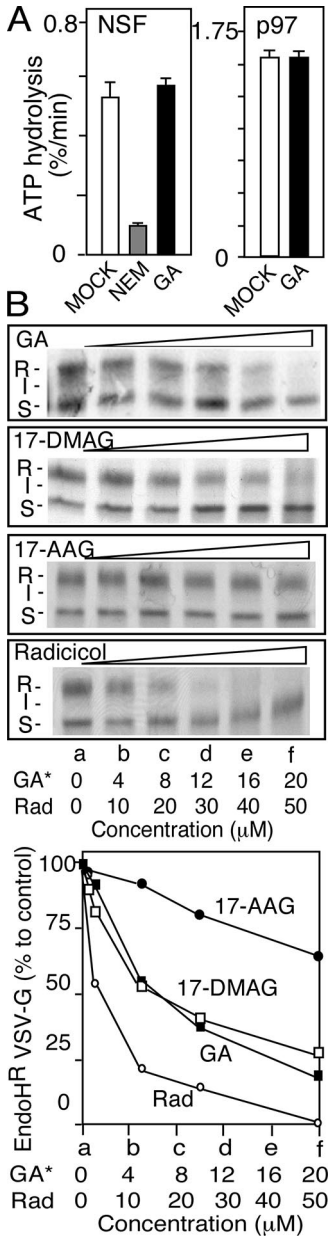

Figure 3. Effect of Hsp90 inhibitors on ER-to-Golgi transport of VSV-G^{ts}. (A) GA does not inhibit NSF or p97 ATPase activity. ATPase activity of NSF or p97 was measured in the absence of presence of GA (50 μM) (see *Materials and Methods*). Quantitation is based on two independent experiments with triplicate samples. Error bars indicate SEM. (B) VSV-G^{ts} transport was measured using a temperature-shift, pulse-chase protocol as described in *Materials and Methods*. After transport, VSV-G^{ts} was immunoprecipitated, samples were digested with endo H and processed for SDS-PAGE. (Top) Shown are autoradiographs of processing intermediates of VSV-G^{ts} formed in the presence of different inhibitors following 30 min of transport at the indicated final concentrations of the indicated inhibitor. After endo H digestion, VSV-G^{ts} migrates on SDS-PAGE as the endo H-sensitive ER glycoform (S); an intermediate early (*cis*/*medial*-) Golgi glycoform (I), or a late (*trans*-) Golgi endo H-resistant mature glycoform (R). (Bottom) The ratio of the R form to total amount of VSV-G^{ts} detected in all glycoforms was quantified and normalized with respect to the vehicle (DMSO) control to show the relative inhibitory effect of Hsp90 inhibitors on ER-to-Golgi transport.

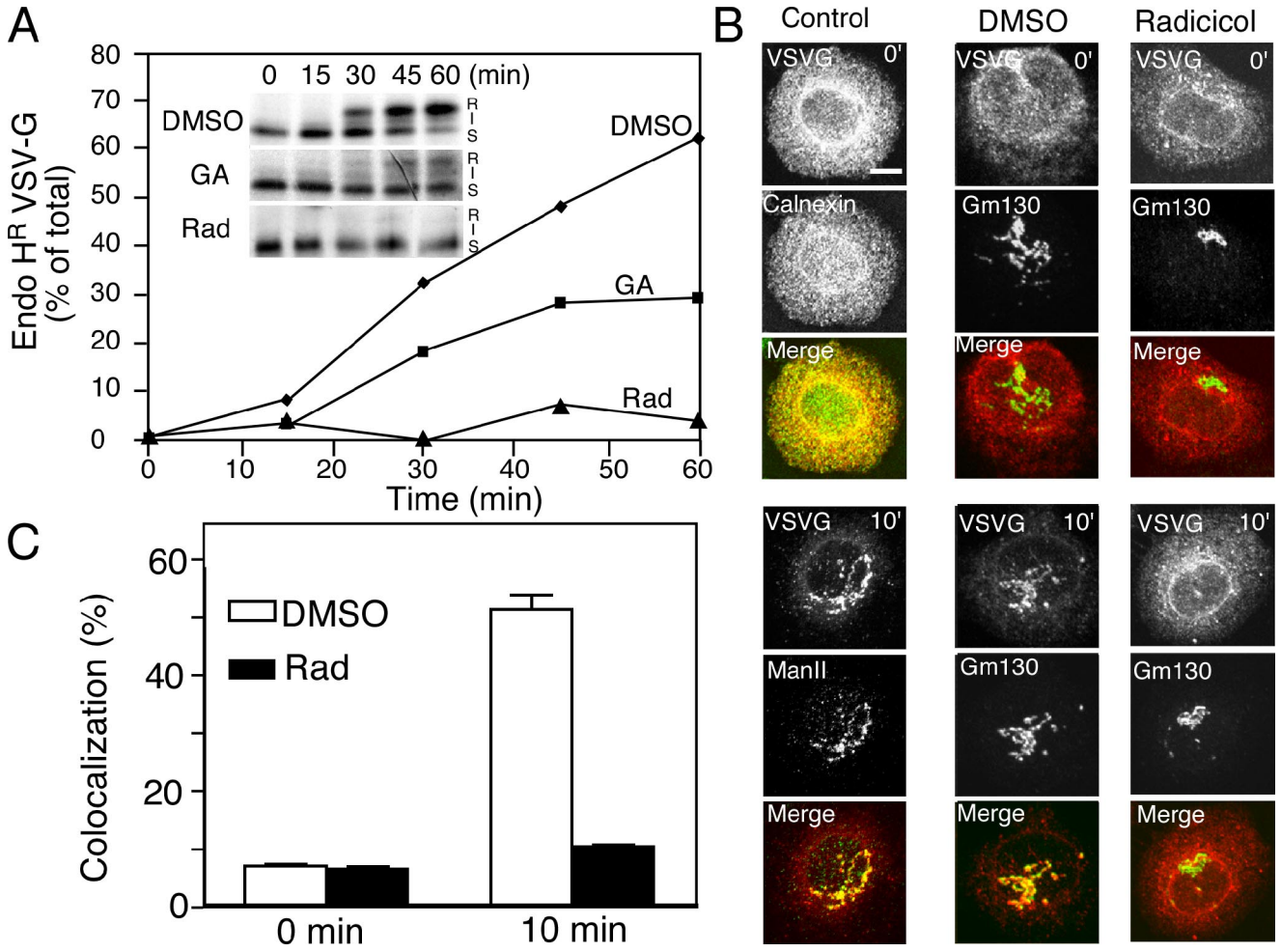

Figure 4. Effect of Hsp90 inhibitors on the kinetics and morphology of VSV-G^{ts} transport to the Golgi. (A) Time course of VSV-G^{ts} transport in the presence of 0.1% DMSO (control), 20 μM GA, or 50 μM radicicol. VSV^{ts}-infected cells were pretreated with drug for 60 min before transfer to the permissive temperature (32°C) to initiate ER export. (B) Morphological analysis of the effect of Hsp90 inhibitors on VSV-G^{ts} transport. Cells were pretreated with radicicol (50 μM) for 30 min at the restrictive temperature (40°C) before temperature shift to initiate ER export for 10 min at 32°C. Marker antibodies: ER, calnexin; *cis/medial*-Golgi, Man II or GM130. Bar, 10 μm. (C) Quantitation of overlap between VSV-G^{ts} and GM130 in Golgi stacks from at least 10 cells at the 0- and 10-min time point in the presence or absence radicicol (see *Materials and Methods*).

In the absence of drug, ~50% of total VSV-G^{ts} protein synthesized during the pulse was processed to the endo H-resistant form by the 30-min time point at 32°C (Figure 3B, band R). Half-maximal inhibition of VSV-G^{ts} maturation by GA and 17-DMAG was observed at ~10 μM, whereas half-maximal inhibition with radicicol was observed at 15 μM. 17-AAG showed only 25% inhibition at 20 μM final concentration. Although GA showed a partial effect (~25%) on protein stability during the 1-h postlabeling incubation period at 40°C in the presence of high concentrations of drug (>25 μM), no effect on stability was observed with the other Hsp90 inhibitors, indicating that the block in transport is not a consequence of targeting of VSV-G^{ts} for degradation when added after synthesis.

Using 20 μM GA and 50 μM radicicol to generate an acute exposure to drug, we found that preincubation for as little as 15 min for both drugs resulted in significant inhibition of VSV-G^{ts} transport, although maximum effects for radicicol were observed after a 30-min preincubation and for GA, a 1-h preincubation period (our unpublished data). Thus, the effects of both drugs on the Hsp90-client interaction involved in membrane trafficking are time-dependent and saturable. In the presence of 20 μM GA or 50 μM radicicol, there was no detectable effect on the steady-state level of GDI in cells (data not shown), indicating that degradation of GDI was not responsible for the observed effects. The concentration of drug required for rapid inhibition of transport could reflect a variety of factors, including solubility of the drug in the medium, nonspecific binding to serum components and rate of uptake by cells for delivery and inactivation of the endogenous Hsp90 pools affecting transport.

Hsp90 Inhibitors Block Both ER-to-Golgi and Intra-Golgi Transport

We next determined the effect of GA and radicicol on the kinetics of VSV-G^{ts} transport from the ER to and through the Golgi. Using a concentration of GA that inhibits transport by ~70% (20 μM) (Figure 3B), GA reduced the kinetics of VSV-G^{ts} transport from the ER to the Golgi with notable accumulation of the band I processing intermediate (Figure 4A, band I) not observed in the control, suggesting that GA inhibits both ER-to-Golgi and intra-Golgi transport. Use of

radicicol at a more acute concentration (50 μM) (Figure 3A) showed inhibition at all time points examined, restricting VSV-G^{ts} to the endo H-sensitive ER form (Figure 4A). These results suggest that loss of appearance of endo H-resistant forms is a consequence of inhibition of ER export and not degradation.

Given its strong effect on processing of VSV-G^{ts} to endo H-resistant forms, the site of action of radicicol was further analyzed by indirect immunofluorescence. In VSV-G^{ts} expressing cells incubated at 40°C, as expected, VSV-G^{ts} distribution completely overlapped with the distribution of calnexin, an ER-associated folding chaperone (Figure 4B, top left). After shift to 32°C, VSV-G^{ts} exits the ER through punctate, peripheral pre-Golgi intermediates (Bannykh *et al*., 1996). By 10 min, VSV-G^{ts} overlaps with the *cis*-Golgi marker GM130 (see below) or the *cis/medial*-Golgi marker α1,2-mannosidase II (Figure 4B, bottom left). A similar result was observed in the present of the DMSO vehicle control (Figure 4B, middle) where VSV-G^{ts} strongly overlapped with GM130 at the 10-min time point. In contrast, preincubation for 1 h in the presence of 50 μM radicicol before temperature shift for 10 min, a condition that inhibits appearance of endo H-resistant VSV-G^{ts} glycoforms (Figure 3B), blocked trafficking to the *cis*-Golgi compartment marked by the distribution of GM130 (Figure 4B, right). Quantitative analysis of overlap of VSV-G^{ts} with GM130 showed that the delivery of VSV-G^{ts} to the *cis*-Golgi compartment was blocked in the presence of radicicol by nearly 10-fold compared with the DMSO vehicle control (Figure 4C). We also observed a marked reduction in trafficking of VSV-G^{ts} to the Golgi in the presence of GA at concentrations >20 μM (our unpublished data). The morphological observations are consistent with the effects of GA and radicicol on the rate of processing of VSV-G^{ts} to endo H-resistant forms (Figure 4A). The combined results suggest that both GA and radicicol block Hsp90-dependent steps in the early secretory pathway, consistent with previous studies that demonstrate that dominant negative Rab1A mutants, which block Rab1 cycling between GDP- and GTP-bound forms, potently inhibit ER-to-Golgi and intra-Golgi transport (Nuoffer *et al*., 1994; Peter *et al*., 1994; Pind *et al*., 1994).

Rab1 Overexpression Can Partially Rescue the Effect of Hsp90 Inhibitors on Transport

Although the above-mentioned results are consistent with the idea that Hsp90 is required for GDI-dependent Rab1 recycling steps in ER-to-Golgi transport, we examined whether the sensitivity of Hsp90-dependent Rab1 recycling could be reduced by increasing the steady-state level of Rab1 in the cell. For this purpose, Rab1 was transiently expressed in CHO cells. If the block in transport were a direct consequence of the inability to recycle Rab1 through GDI–Hsp90 client chaperone interactions, then overexpression of Rab1 would be anticipated to attenuate the drug effect by increasing the general Rab1 pool available for normal function.

Using a pulse-chase protocol, we first examined the level of processing of VSV-G^{ts} to the endo H resistant form at the 30-min time point in either absence or the presence of 40 μM radicicol, a concentration that inhibits transport by ~95% (Figure 3B). In the mock control, ~25% of the total VSV-G^{ts} was transported to the Golgi and processed to the endo H-resistant form (Figure 5A, lane 1, top); radicicol reduced transport to <5% of total (Figure 5A, lane 1, bottom). Overexpression of wild-type Rab1B ~10-fold higher than endogenous level (Figure 5C) did not increase the endogenous rate of transport in the absence of the radicicol (Figure 5A, lane 2, top) since the amount of endo H-resistant VSV-G^{ts} was similar to that observed in the DMSO vehicle control (Figure 5A, lane 1, top). This result is consistent with previous observations that overexpression of wild-type Rab1B has no effect on the kinetics of transport of VSV-G^{ts} to the Golgi (Tisdale *et al*., 1992). In contrast, whereas in the presence of 40 μM radicicol VSV-G^{ts} processing to the endo H-resistant form was reduced by ~75% (Figure 5A, lane 1, bottom), in the presence of overexpressed Rab1B transport was reduced by only 20–30% of the value observed in the radicicola-treated cells (compare Figure 5A, lane 2, top to Figure 5A, lane 2, bottom). In Figure 5B, we normalized the amount of endo H-resistant band observed in the mock control (Figure 5A, lane 1, bottom) to that observed in the presence of Rab1b (Figure 5A, lane 2, bottom). Quantitatively, we observed a statistically significant 50% increase in response of ER-to-Golgi transport by the overexpression of Rab1B in the presence of radicicol (Figure 5A, lane 2, bottom). To determine whether rescue was specific for overexpression of Rab1B, we compared its effect to that of Rab3A, a GTPase that is specific for synaptic vesicle fusion (Sudhof, 2004), and Sar1A, which facilitates COPII vesicle formation (Kuge *et al*., 1994; Aridor *et al*., 1998). Under identical expression conditions, neither Rab3A nor Sar1A overexpression (Figure 5C) rescued the

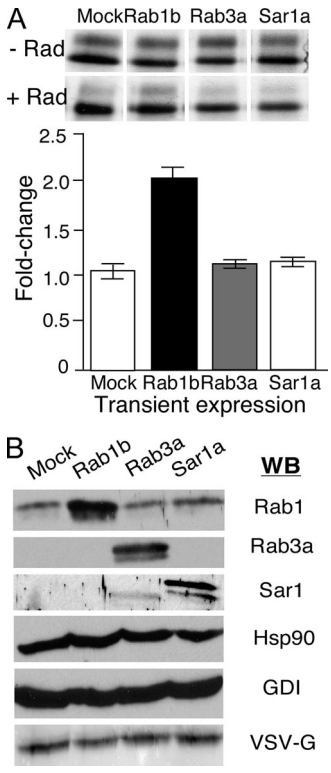

Figure 5. Overexpression of Rab1 protein antagonizes the inhibitory effect of radicicol on VSV-G^{ts} transport. (A) CHO-K1 cells were transfected with pcDNA3.1 plasmids containing Rab1B, Rab3A, Sar1A, or empty vector 24 h before infection with VSV^{ts} as described in *Materials and Methods*. Infected cells were then pulse-labeled in the absence or presence of radicicol (Rad). Representative autoradiograph is shown. (B) Quantitation based on two independent experiments with triplicate samples. Reported as percentage of increase in endo H-resistant VSV-G^{ts} normalized to mock control to illustrate fold-difference in recovery. (C) Immunoblot analysis of transfected cell lysates demonstrating expression of each of the GTPases relative to endogenous levels. Transient expression did not significantly affect the endogenous level of Hsp90, GDI or alter the total amount of VSV-G^{ts} synthesized.

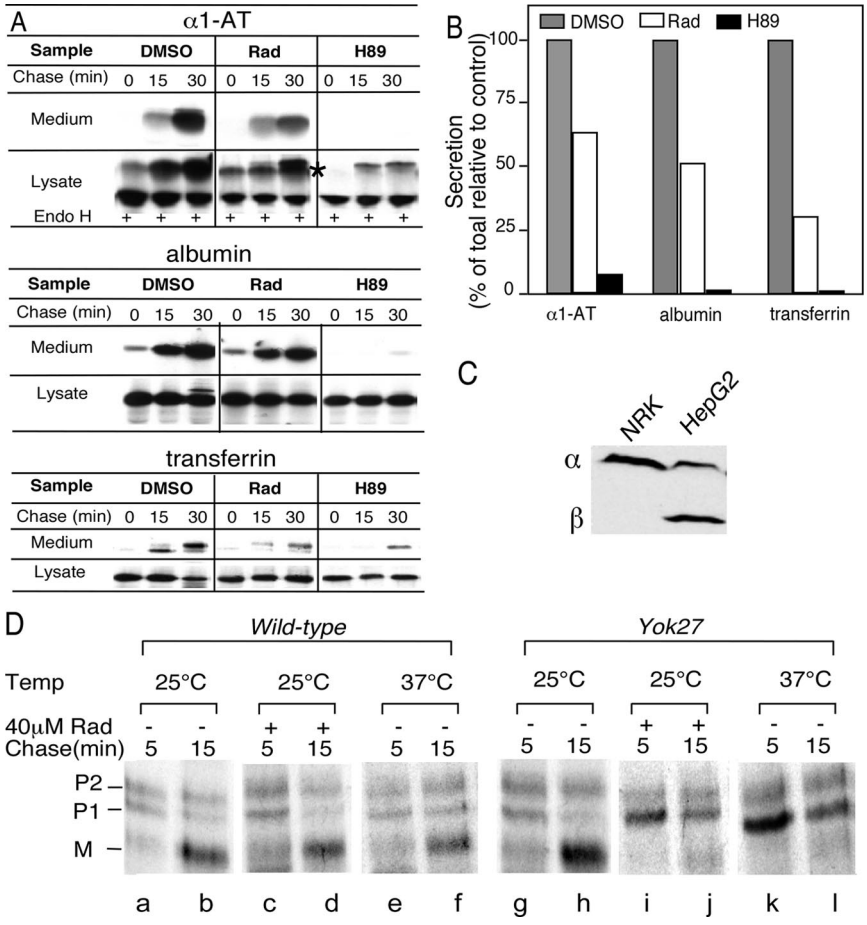

Figure 6. Hsp90 activity is required for general protein secretion. (A) HepG2 cells were pulse-labeled in the presence of 0.1% DMSO, 50 μM radicicola, or 50 μM H89 (Aridor and Balch, 2000) and chased for indicated amount of time to follow processing of α1-AT to endo H-resistant form in cell lysates (α1-AT), or secretion into the medium of (α1-AT, albumin, and transferring) as described in *Materials and Methods*. (B) Quantitation of immunoblots at the 30-min time point for each marker protein reported as percentage of vehicle (DMSO) control. (C) Immunoblot of α/βGDI in NRK and HepG2 lysates. Equivalent total cell lysate protein loaded in each lane. The αGDI polyclonal antibody is ~100-fold more sensitive to αGDI compared with βGDI based on titration with recombinant protein (our unpublished data), indicating that HepG2 GDI pool is predominately (>98%) βGDI. (D) Transport of CPY in the Yok27 Hsc82 mutant strain. Parent wild type (left) or Yok27 mutant strains were incubated at the indicated temperatures in the absence or presence of 40 μM radicicol for 12–16 h to inactivate the abundant Hsp90 pool. Transport of CPY from the ER (P1) form to the Golgi (P2) and mature (M) vacuolar forms was measured using the pulse-labeling protocol described in *Materials and Methods*. Typical result from three independent experiments is shown.

inhibitory secretion of VSV-G^{ts} caused by radicicol (Figure 5A, lanes 3 and 4). These results suggest that the radicicol-sensitive step in ER-to-Golgi transport is sensitive to the steady level of Rab1 GTPase function in the early secretory pathway.

Hsp90 Inhibitors Block Secretion of Endogenous Proteins

Although the above-mentioned results largely focus on trafficking of VSV-G^{ts}, it remained possible that inhibition is a consequence of stress-induced VSV^{ts} infection. Therefore, we examined the effects of the Hsp90 inhibitors on secretion of three endogenously secreted proteins: α1-AT, albumin, and transferrin in a HepG2 liver cell line.

Cells were pulse-labeled in the presence of 50 μM radicicola, and the level of each protein secreted into the medium was quantitated as the percentage of total protein synthesized during the pulse. Secretion of all three markers to the medium was potently blocked by the rapid acting inhibitor H89, which prevents COPII vesicle formation required for ER export (Aridor and Balch, 2000) (Figure 6A, top; quantitation in B). Exposure of cells to radicicol for 45 min during the pulse-labeling period, in contrast to VSV-G^{ts}, had no effect on the total recovery of α1-AT, albumin, or transferrin during the chase period, indicating that the lumenal Hsp90-like chaperone GRP94 is unlikely to play a role in their folding or stability (Figure 6A). However, the rates of secretion of α1-AT and albumin to the medium were reduced by approximately twofold, whereas transferrin secretion was reduced by fourfold (Figure 6, A and B). Because α1-AT has two *N*-linked carbohydrates, we used acquisition of endo H resistance to determine the effect of radicicol on ER-to-Golgi trafficking. In agreement with the effect of the drug on inhibiting secretion to the medium, processing to endo H resistance forms was reduced by approximately twofold (Figure 6, A and B). Moreover, reduction in transport of α1-AT coincided with the accumulation of an endo H-resistant Golgi-processing intermediate reflecting retarded trafficking through the Golgi (Figure 6A, asterisk). The inhibition observed for all three soluble marker proteins lead us to conclude that general protein transport to and through the Golgi is affected by Hsp90 inhibitors. This is consistent with the general importance of GDI-dependent Rab1 recycling pathways for transport of both membrane and soluble cargo (Gurkan *et al*., 2005). Interestingly, HepG2 cells principally express βGDI (Figure 6C). This is in contrast to other cell types, including NRK (Figure 6C) as well as CHO, baby hamster kidney, HeLa, human embryonic kidney 293, and COS cells (our unpublished data) which, surprisingly, principally express the α isoform of GDI. These results suggest that the more ubiquitously expressed βGDI isoform (Gurkan *et al*., 2005) also may use Hsp90 for recycling of Rab GTPases.

To determine whether yeast display a similar requirement for Hsp90 in Rab recycling in export of soluble cargo from the ER, we examined the effects of Hsp90 inhibitors on transport of CPY, a soluble vacuolar protease. CPY shows distinct molecular weight differences on SDS-PAGE as it is sequentially processed from its ER-specific P1 form to the Golgi-specific P2 form and the vacuole-specific mature (M) form (Figure 6D). Compared with mammalian cells, yeast are largely insensitive to various Hsp90 inhibitors due to the

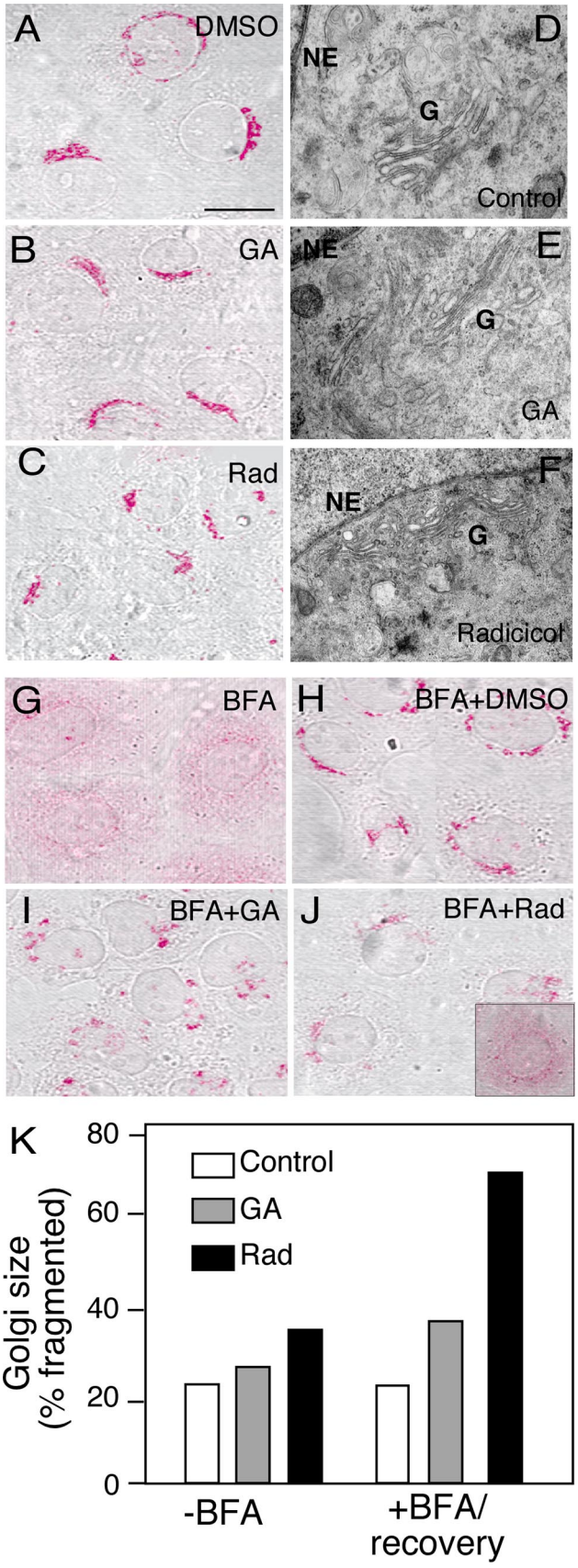

Figure 7. GA and radicicol prevent the recovery of Golgi compartments after treatment with BFA. (A) NRK cells were treated with vehicle (0.1% DMSO) control (A and D), 20 μM GA (B and E), or 50 μM radicicol (Rad) (C and F) at 37°C for 2 h before preparation for indirect immunofluorescence using the Golgi specific antibody Man II (A–C) or electron microscopy (D–F) (NE, nuclear envelope; G, Golgi). (G–K) Cells were treated with 2.5 μg/ml BFA for 1.5 h in the absence (G) or presence of DMSO (H), 20 μM GA (I), or 50 μM radicicol (J) and either transferred to ice (G) or incubated for an additional 30 min in the absence of BFA, but in the presence of the indicated Hsp90 inhibitor. Inset in J illustrates that Rad does not prevent BFA-induced collapse of the Golgi into the ER. In K, the percentage of residual fragmented Golgi relative to the control incubation was determined by the ratioing the area of the punctate Golgi staining regions that occupied <5 μm^2 (indicative of fragmented structures) to the total Golgi area labeled by Man II (20 cells for each condition were quantitated using NIH ImageJ software).

presence of a highly abundant Hsp90 homologue (Hsc82) pool (5% of total protein) and active efflux systems. As expected, addition of each of the Hsp90 inhibitors at the highest concentrations tested for mammalian cells to wild-type yeast had no effect on CPY transport at either 25 or 37°C (Figure 6D, a–f). We next examined three yeast Hsc82 temperature-sensitive mutant strains: Yok5, Yok25, and Yok27. Yok5 (G170D) and Yok25 (A97T) have been shown to reduce glucocorticoid receptor activity when expressed heterologously (Nathan and Lindquist, 1995). Transport of CPY in Yok5 and Yok25 mutant strains was insensitive to both GA and radicicol at the permissive temperature (25°C). In contrast, following incubation at 37°C, both strains showed significant inhibition of transport and processing of CPY to the mature vacuolar form (our unpublished data). Because the inhibition observed at 37°C could reflect a variety of Hsp90-sensitive client interactions, we took advantage of a point mutation (T101I) in the Yok27 strain that reduces the ATPase activity of Hsc82 in vitro and renders yeast hypersensitive to radicicol and GA (Kimura *et al.*, 1994; Nathan and Lindquist, 1995; Piper *et al.*, 2003). Cells were cultured at either the permissive (25°C) or restrictive (37°C) temperatures before pulse labeling to follow CPY transport. In contrast to the wild-type strain parent strain, which showed no inhibition of CPY transport in the absence or presence of radicicol at 25 or 37°C (Figure 6D, a–f), processing of CPY to the p2 Golgi form and the M vacuolar form in the Yok27 mutant strain was sensitive to radicicol at 25°C (Figure 6D, g–j). This result was analogous to that observed after transfer of Yok27 to the restrictive temperature (37°C) (Figure 6D, k and l). Identical results were observed with GA (our unpublished data). The chemical synthetic effect of GA and radicicol on the ability of the Yok27 mutant allele at the permissive temperature (25°C) to inhibit transport of CPY emphasizes the possibility that Hsc82, like Hsp90 in mammalian cells, is involved in recycling of Rab GTPases.

Hsp90 Inhibitors Block Golgi Reassembly after Treatment with BFA

Although Hsp90 inhibitors block ER-to-Golgi and intra-Golgi transport of cargo (Figures 3, 4, and 6), it needed to be established whether these inhibitors only effect cargo transport, or in addition, affect Golgi organization. We have previously demonstrated that Golgi structure is dependent on Rab1 function because overexpression (Nuoffer *et al.*, 1994) or microinjection (Wilson *et al.*, 1994) of Rab1 dominant negative GDP-restricted mutants that prevent Rab1 activation trigger Golgi fragmentation. A block in normal Rab1 recycling by Hsp90 inhibitors could recapitulate a similar effect on Golgi structure depending on the kinetics of

Golgi instability in response to Rab1 dysfunction, thereby indirectly inhibiting Rab1-dependent vesicular transport steps mobilizing cargo from the ER to and through the Golgi.

We first examined the effect of acute exposure to GA and radicicol on Golgi structure after a 2-h incubation in the presence of each drug, the duration of most transport experiments (Figures 3, 4, and 6). Compared with the DMSO vehicle control, the presence of either 20 μM GA or 50 μM radicicol during this time period had no effect on Golgi morphology based on by staining for the *medial*-Golgi marker Man II (Figure 7, A–C) or electron microscopy (Figure 7, D–F). However, longer term incubation in the presence of drugs (>8 h) resulted in extensive Golgi fragmentation and cell death (our unpublished data; see below). These results suggest that the inhibition of VSV-G^{ts} transport by a short incubation (2 h) in the presence of Hsp90 inhibitors is unlikely to trigger global disassembly of the Golgi stack. Thus, the primary initial effect of Hsp90 inhibitors is to inhibit more rapid Rab1-dependent vesicular trafficking pathways controlling the continuous flow of cargo from the ER and through sequential Golgi compartments.

Given the observation that the Golgi stack undergoes fragmentation after exposure to GA and radicicol for >8 h, we tested the possibility that an Hsp90-dependent step involving Rab1 recycling is required for assembly and maintenance of Golgi structure. For this purpose, we analyzed the effect of Hsp90 inhibitors on Golgi recovery after treatment of cells with BFA. Incubation with BFA triggers collapse of Golgi processing enzymes into the ER (Lippincott-Schwartz *et al*., 1989). We have recently shown that recovery of intact Golgi stacks following BFA washout is Rab1-dependent (Bannykh *et al*., 2005). To examine whether Golgi recovery in response to BFA was dependent on Hsp90, cells were treated with BFA at 37°C for 90 min to collapse the Golgi to the ER followed by a 30-min recovery in the absence of BFA to regenerate the stacked structure. To ensure substantial inactivation of the Hsp90 pool, Hsp90 inhibitors were added at the time of addition of BFA. In the DMSO vehicle control, as expected, the Golgi marker Man II was found in a dispersed ER distribution after incubation in the presence of BFA (Figure 7G). Identical results were observed in cells treated with BFA in the presence of either GA or radicicol, indicating that Hsp90-sensitive steps are not involved in the rapid Golgi collapse to the ER after BFA treatment (Fig. 7J, inset). After BFA washout, in the presence of DMSO, Man II was recovered in normal Golgi stacks that form the typical perinuclear ribbon-like structure (Figure 7H). In contrast, when GA and radicicol were incubated with cells during the recovery period, we noted significant inhibition of reassembly of the Golgi apparatus (Figure 7J). In both cases, Golgi elements remained in small punctate structures distributed throughout the cell cytoplasm. We quantitated the extent of residual Golgi fragmentation remaining in GA and radicicol treatment cells by ratioing the total area of Man II staining structures in each cell to those in which Man II was found in dispersed, small punctate structures that occupied <5-μm^2 measured total surface area. We observed that in absence of drug during BFA recovery, small punctate Golgi structures comprised <20–25% of the total Man II-positive compartments (Figure 7K). This value was increased to 35 and 73% for BFA recovery in the presence of GA and radicicol, respectively (Figure 7K). The more extensive fragmentation observed with radicicol is consistent with its more potent inhibition of cargo trafficking (Figures 3, 4, and 6) and Rab recycling (Figure 2) at the concentrations tested. Thus, inhibition of Hsp90 function prevents Rab1-dependent trafficking events required for maturation and reassembly of the central Golgi stack (Bannykh *et al*., 2005).

DISCUSSION

We have provided a number of distinct lines of evidence that the recycling activity of the Rab1 GTPase involved in ER-to-Golgi transport is likely regulated by a Hsp90 chaperone complex. In support of this conclusion, we recovered GDI from Golgi membranes in a Rab1- and Hsp90-containing complex and a cytosolic complex composed of Hsp90 and GDI. In addition, the Hsp90-specific inhibitors GA, 17-DMAG, and radicicol exerted strong effects on trafficking of VSV-G^{ts} and endogenous secreted cargo from the ER to the Golgi in the both mammalian cells and yeast, on Rab1-dependent Golgi assembly, and, specifically, on GDI-dependent Rab1 extraction in vitro. We observed no effect of either GA or radicicol on the ATPase activity of either NSF or p97 in vitro at concentrations which, when added exogenously to cells, inhibit VSV-G^{ts} transport and Golgi reassembly. These results suggest that Hsp90 inhibitors do not interfere with known ATPases involved in membrane trafficking, a result consistent with the specificity of both GA and radicicol for Hsp90–client interactions (Prodromou and Pearl, 2003). The recognition that two different Rab GTPases of highly divergent function (Rab1 in constitutive Golgi trafficking [this study] and Rab3A in regulated secretion at the synapse [Sakisaka *et al*., 2002]) both use a Hsp90 chaperone system for function lead us to suggest that general Rab recycling may be controlled by Hsp90.

GDI–Hsp90 Complexes

Consistent with the idea that Hsp90 is required for Rab1-dependent recycling, we detected a complex containing Hsp90, GDI, and Rab1 on membranes of an enriched Golgi fraction. The GDI-Rab1–containing pool was small (1%) relative to the total Hsp90 pool on Golgi membranes reflecting the expected rapid dynamics of Hsp90-dependent client pathways, the rapid dynamics of membrane trafficking pathways, and the fact that up to 15 different Rabs may be involved in different aspects of Golgi trafficking (Gurkan *et al*., 2005). Given that the Hsp90 chaperone cycle requires a variety of cochaperones whose recruitment and association with the client substrate are initiated through Hsp70/Hsp40 (steroid hormone receptors) or Cdc37 (signaling kinases) (Pratt and Toft, 2003; Pratt *et al*., 2004), our results suggest that a membrane-anchored cochaperone component is likely to be required for localization of an Hsp90–GDI complex to Golgi membranes. In support of this view, in the synapse we have identified the abundant cysteine string protein (CSP) as the potential membrane-anchored J-domain containing Hsp40 present on synaptic vesicles that could mediate αGDI localization for recycling of Rab3A (Sakisaka *et al*., 2002). Interestingly, CSP along with α-synuclein seem to facilitate SNARE assembly at the synapse, suggesting that all of these components may function coordinately as part of a Rab3A regulated hub regulating neurotransmitter release (Chandra *et al*., 2005; Gurkan *et al*., 2005). Of high interest are other members of the J-domain family of proteins (e.g., Hdj-2) that contain membrane anchors and localize to the Golgi. These may facilitate coupling Hsp90 to GDI. The association of GDI with Golgi membranes through Hsp90 is consistent with the need for a Rab1-independent mechanism involving the MEL domain on GDI (Luan *et al*., 1999), and the results presented herein that cargo trafficking in yeast through the Golgi can be rendered sensitive to GA/radicicol in the

Yok27 mutant strain at the permissive temperature. We also observed a cytosolic pool of GDI interacting with Hsp90 that lacked Rab1. This may be a transient intermediate in the recycling pathway. Consistent with this interpretation, recovery of the Hsp90–GDI client complex from cytosol was enhanced by the addition GA.

Specificity of Effect of GA on Rab1 Recycling

To demonstrate that Hsp90 is specifically required for Rab1–GG recycling, we examined the effects of Hsp90 inhibitors using a well established biochemical assay that measures directly the ability of Rab1 to be retrieved from Golgi membranes using recombinant αGDI (Peter *et al*., 1994). Similar to results observed in the in vitro extraction of Rab3A from synaptic membranes (Sakisaka *et al*., 2002), we found that retrieval was sensitive to both GA and radicicol. The data provide strong support for the view that αGDI-dependent Rab1 retrieval is sensitive to Hsp90 function. Because inhibition of retrieval required pretreatment of cells with GA in vivo before perforation and extraction, these results are consistent with the interpretation that an Hsp90-dependent priming event(s) is required for membrane retrieval of Rab1. Interestingly, the inhibitory effect of radicicol on VSV-G^{ts} transport could be partially restored by overexpression of Rab1B but not by other GTPases such as Rab3A that regulates synaptic vesicle fusion, nor by Sar1, a GTPase that mediates COPII coat assembly/disassembly. These results provide an additional line of evidence for the proposed specific role of Hsp90 in GDI-dependent Rab1-dependent Golgi trafficking events.

Effect of Hsp90 Inhibitors on Membrane Traffic and Golgi Organization

To evaluate the effect of Hsp90 inhibitors on membrane traffic through the early exocytic pathway, we examined their effect on transport of VSV-G^{ts} to the Golgi using both biochemical and morphological approaches. Biochemically, GA, 17-DMAG and radicicol perturbed processing of VSV-G^{ts} to endo H-resistant forms and led to the appearance of Golgi-processing intermediates indicative of inhibition of not only ER-to-*cis*-Golgi trafficking but also inhibition of intra-Golgi (*cis*-to-*trans*) transport. This is consistent with the idea that the Golgi is compartmentalized with Golgi processing enzymes enriched in distinct compartments along a *cis*-, *medial*-, and *trans*-axis that require Rab-dependent activities for transit of cargo. These biochemical results were confirmed morphologically where radicicol largely prevented transit of VSV-G^{ts} into the Golgi stack at a concentration that inhibited processing of VSV-G^{ts} to endo H-resistant structures. Interestingly, using short, acute treatments with Hsp90 inhibitors to inhibit transport (2 h), we did not observe a major disruption of Golgi structure, a phenotype that can be triggered rapidly by perturbing Rab1 function through microinjection of Rab1 dominant negative (Rab1 DN) mutants (Wilson *et al*., 1994) or by addition of the drug BFA (<15 min) (Lippincott-Schwartz *et al*., 1989). However, we have found that both GA and radicicol do manifest fragmentation effects on Golgi organization after longer incubation periods (>8 h), consistent with the need for Rab1 function for the steady-state maintenance of Golgi structure (Nuoffer *et al*., 1994; Wilson *et al*., 1994). The fact that addition of GA and radicicol require 15 min to 1 h to manifest inhibition of trafficking in vivo without perturbing Golgi structure suggests that Hsp90 inhibitors do not share the same immediate target as Rab1 DN mutants or BFA, the latter known to inactivate Arf1-specific GEFs. Because Rab GTPases seem to be functionally in excess (Alory and Balch, 2000, 2003) significant inhibition (>90%) of Hsp90-GDI dependent recycling function would be required to elicit trafficking responses regulated by Rab1 and, potentially, other Golgi localized Rabs. Therefore, the rate of onset of inhibition is likely to reflect the need to first inactivate the large (2–3% of total cytosol) pool of Hsp90 contributing to recycling. This interpretation is consistent with our observations that overexpression of Rab1 altered the sensitivity to radicicol, possibly reflecting the fact that excess Rab1 may reduce the demand on recycling pathways for normal function.

Dosage Effect

It is known that GA, GA derivatives, and radicicol have nanomolar affinities for purified Hsp90 in vitro (Roe *et al*., 1999) but that they display a wide range of dosage effects (nanomolar to micromolar) when applied to cell-based assays measuring Hsp90-client dependent folding and signaling pathways (Kamal *et al*., 2003). This discrepancy undoubtedly reflects the pharmacodynamics of these drugs for each client. The dose required to inhibit cell proliferation using assays that typically measure growth over a 24- to 96-h period (50 nM–1 μM) is well below the values that we have applied to inhibit ER-to-Golgi transport within a short time frame, where we observe half-maximal inhibition from 10 to 15 μM for GA, 17-DMAG, and radicicol. By applying a much higher extracellular concentration, we are likely to generate a more rapid increase in the intracellular inhibitory pool that is necessary to acutely interfere with Hsp90 function. We focused on acute affects (<1–2 h) to avoid global perturbation of membrane organization in response to inhibition of cell proliferation through known GA-sensitive kinase signaling pathways (Bagatell and Whitesell, 2004). A number of factors could affect the concentration of inhibitor required for acute biological inhibition of membrane trafficking. These include how fast an individual inhibitor is either taken up and/or metabolized by a given cell type, the accessible pool of trafficking components available for inhibition, and the potential differential sensitivity of free Hsp90 compared with different Hsp90-dependent client complexes to these inhibitors. In the later case, recent studies have demonstrated that the higher affinity targets for Hsp90 inhibitors seem to be those pools of Hsp90 engaged in client complexes, particularly abundant in rapidly proliferating cancer cells (Kamal *et al*., 2003). Further analyses using a variety of cell types with different levels of endogenous Rab1 may help to clarify the pharmacodynamics of Hsp90 inhibitors on membrane trafficking.

Role of Signaling Kinases in Hsp90-GDI–dependent Rab Recycling

Signaling kinases are frequently found to be Hsp90 clients (Pratt and Toft, 2003; Prodromou and Pearl, 2003; Roe *et al*., 2004). Recycling of Rab5 by GDI is regulated by phosphorylation through the p38 mitogen-activated protein (MAP) kinase signaling pathway (Cavalli *et al*., 2001). By two-dimensional gel analysis, we have been unable to detect a significant change in the level of phosphorylated GDI in control cells compared with those of Hsp90 inhibitor-treated cells (our unpublished observations), a result similar to our observation that Hsp90-dependent neuronal αGDI recycling of Rab3A is insensitive to p38 MAP kinase inhibitors (Sakisaki *et al*., 2002). Although p38 MAP kinase is currently not recognized as an Hsp90-client substrate, regulation of GDI function by phosphorylation does raise the possibility that currently unknown Hsp90-dependent kinase signaling pathways could transiently regulate the formation of GDI–Hsp90 complexes that facilitate Rab1 or Rab3A retrieval.

Role of Hsp90-dependent GDI Rab Retrieval during Endocytosis

Although we have focused on the role of Hsp90 in GDI-dependent Rab1 retrieval in the exocytic pathway, it is evident that inhibition of endocytic recycling of signaling receptors could also be affected. For example, recent studies have shown that low concentrations (1 μM) of GA do not necessarily inhibit ErbB2 tyrosinse kinase internalization involved in proliferation of breast cancer cells; rather, they redirect ErbB2 sorting in the endosome to the lysosome for degradation (Austin *et al*., 2004). Similar results have been reported for CD14 (Vega and De Maio, 2003). We have examined the acute effects of GA (30-min exposure) on general fluid phase endocytosis and transferrin receptor (Tfn-R) recycling, an abundant recycling receptor that is crucial for uptake of the serum protein transferrin. Although we observed no effect on fluid phase endocytosis, nor the rate of internalization of Tfn-R, 10 μM GA strikingly prevented the recycling Tfn-R from the endosome to the cell surface (our unpublished observations). One possibility is that GA may alter or inhibit maturation of Hsp90 GDI-dependent Rab endosomal sorting pathways leading to Rab conversion (Rink *et al*., 2005).

Role of Hsp90 and GDI in Cell Proliferation

Hsp90 modulates signaling kinase pathways controlling cell proliferation (Pratt and Toft, 2003; Prodromou and Pearl, 2003) and the activity of several oncogenes, including Her-2/ErbB2, Akt, Raf-1, Bcr-Abl, mutated p53, and v-*Src* (Maloney and Workman, 2002). Interestingly, because Hsp90–client complexes in cancer cells are now thought to have a higher sensitivity for Hsp90 inhibitors than uncomplexed Hsp90 in normal cells (Kamal *et al*., 2003), it has been proposed that these activated pathways are the target of Hsp90 inhibitors 17-DMAG and 17-AAG that are currently in clinical trails. 17-DMAG showed a similar profile of trafficking inhibition as GA. It is now evident that a reduction in transport through the exocytic pathway would also be expected to have a pronounced impact on the growth rate of rapidly proliferating cells.

A Model for Hsp90 Function in Rab Recycling Pathways

Our results demonstrating biochemically and morphologically that Hsp90 is required for Rab1 recycling is consistent with a recent extensive network analysis of Hsp90 interactions in yeast (Zhao *et al*., 2005). These studies suggest that at least two Rab proteins, Ypt6 (Golgi) and Ypt7 (endosome), are either direct or indirect interacting partners with Hsp90 (Zhao *et al*., 2005). Moreover, conserved oligomeric complexes (COGs), components of Rab-regulated tethering and fusion hubs, also show interaction with Hsp90. We suggest these interactions may reflect the role of Hsp90 in general GDI-dependent Rab recycling in the maintenance of trafficking pathways and Golgi structure.

Why does GDI-dependent Rab1 recycling require Hsp90? One possibility is the need to deliver the highly hydrophobic geranylgeranyl (GG) lipids localizing Rab GTPases to the membrane to the domain II GG binding pocket found in GDI (Schalk *et al*., 1996; Rak *et al*., 2003; Pylypenko *et al*., 2006). GDI is a two-domain protein in which domain I binds the Rab effector region and domain II forms a helical tripod structure that binds GG lipids attached to Rab GTPase at their C terminus (Luan *et al*., 1999; Luan *et al*., 2000; Alory and Balch, 2001, 2003; Rak *et al*., 2003). Domain II exists in two configurations: in the absence of Rab it is in a closed configuration in which the helices are tightly packed (Schalk *et al*., 1996); in the open configuration it forms a deep binding pocket for insertion of GG lipids (Rak *et al*., 2003; Pylypenko *et al*., 2006). By analogy to the SHR-chaperoned pathway, we now propose a model (Figure 8) where sequential steps involving the recruitment of cytosolic GDI (domain II closed configuration) to the lipid bilayer via an Hsp90 intermediate leads to a conformational change in GDI resulting in the formation of the domain II open configuration. The open configuration facilitates transfer of Rab prenyl groups from the lipid bilayer to the domain II lipid binding pocket, resulting in release of the GDI-Rab-GG into the cytosol and dissociation of the Hsp90 complex (Figure 8). In this model, the role of Hsp90 would be to provide a thermodynamically and/or kinetically favorable state for transfer of GG lipids from the bilayer to GDI domain II. Thus, by analogy to recognition of steroid hormone by steroid hormone receptor, Rab-GG is the substrate for the Hsp90–GDI client chaperone complex (Pratt and Toft, 2003; Prodromou and Pearl, 2003). This interpretation is supported by our observation that residues in the domain II GG-binding pocket are essential for Rab extraction (Luan *et al*., 1999; Luan *et al*., 2000; Alory and Balch, 2001, 2003). Such a general model for GDI-dependent Rab recycling provides a mechanism to regulate the extent and rate of recycling through numerous Hsp90 cochaperone activities that may play unanticipated roles in modulating general membrane architecture and function of eukaryotic cells and in response to cell surface signaling pathways.

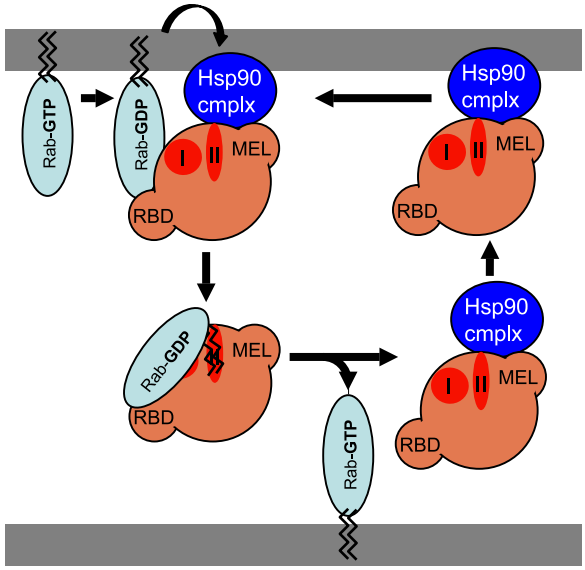

Figure 8. Model for the role of Hsp90 in GDI-dependent Rab recycling pathways. Shown is a model describing the potential role of Hsp90 in GDI-dependent Rab recycling. Hsp90 and its cochaperone machinery are proposed to facilitate the recruitment of GDI to the membrane through MEL, configuring GDI in the domain II open configuration. After hydrolysis of Rab (GTP) to form Rab (GDP), GDI binds the Rab effector domain through domain I. This facilitates transfer of GG lipids from the lipid bilayer to the domain II GG binding pocket, resulting in release of the GDI–Rab (GDP) complex into the cytosol and dissociation from Hsp90. *Discussion* for details.

ACKNOWLEDGMENTS

We thank Dr. Malcom Wood and Dr. Theresa Fassel for assistance in electron microscopy (EM) images and Dr. Atanas Kouov for assisting in EM sample preparation. We thank Drs. K. Tanaka and S. Lindquist for providing yeast

strains, Dr. S. Whiteheart for providing recombinant NSF, Dr. M. Latterich for providing recombinant p97, and Dr. Dan Santi (Kosan, San Francisco, CA) for providing 17-AAG and 17-DMAG. This is TSRI manuscript 7865. The work is supported by National Institutes of Health Grant GM-33301.

REFERENCES

Allan, B. B., Moyer, B. D., and Balch, W. E. (2000). Rab1 recruitment of p115 into a cis-SNARE complex: programming budding COPII vesicles for fusion. Science *289*, 444–448.

Alory, C., and Balch, W. E. (2000). Molecular basis for Rab prenylation. J. Cell Biol. *150*, 89–103.

Alory, C., and Balch, W. E. (2001). Organization of the Rab-GDI/CHM superfamily: the functional basis for choroideremia disease. Traffic *2*, 532–543.

Alory, C., and Balch, W. E. (2003). Molecular evolution of the Rab-escort-protein/guanine-nucleotide-dissociation-inhibitor superfamily. Mol. Biol. Cell *14*, 3857–3867.

An, Y., Shao, Y., Alory, C., Matteson, J., Sakisaka, T., Chen, W., Gibbs, R. A., Wilson, I. A., and Balch, W. E. (2003). Geranylgeranyl switching regulates GDI-Rab GTPase recycling. Structure *11*, 347–357.

Aridor, M., and Balch, W. E. (2000). Kinase signaling initiates coat complex II (COPII) recruitment and export from the mammalian endoplasmic reticulum. J. Biol. Chem. *275*, 35673–35676.

Aridor, M., Weissman, J., Bannykh, S., Nuoffer, C., and Balch, W. E. (1998). Cargo selection by the COPII budding machinery during export from the ER. J. Cell Biol. *141*, 61–70.

Austin, C. D., De Maziere, A. M., Pisacane, P. I., van Dijk, S. M., Eigenbrot, C., Sliwkowski, M. X., Klumperman, J., and Scheller, R. H. (2004). Endocytosis and sorting of ErbB2 and the site of action of cancer therapeutics trastuzumab and geldanamycin. Mol. Biol. Cell *15*, 5268–5282.

Bachner, D., Sedlacek, Z., Korn, B., Hameister, H., and Poustka, A. (1995). Expression patterns of two human genes coding for different Rab GDP-dissociation inhibitors (GDIs), extremely conserved proteins involved in cellular transport. Hum. Mol. Genet. *4*, 701–708.

Bagatell, R., and Whitesell, L. (2004). Altered Hsp90 function in cancer: a unique therapeutic opportunity. Mol. Cancer Ther. *3*, 1021–1030.

Balch, W. E., Dunphy, W. G., Braell, W. A., and Rothman, J. E. (1984). Reconstitution of the transport of protein between successive compartments of the Golgi measured by the coupled incorporation of N-acetylglucosamine. Cell *39*, 405–416.

Balch, W. E., and Rothman, J. E. (1985). Characterization of protein transport between successive compartments of the Golgi apparatus: asymmetric properties of donor and acceptor activities in a cell-free system. Arch. Biochem. Biophys. *240*, 413–425.

Bannykh, S. I., Plutner, H., Matteson, J., and Balch, W. E. (2005). The role of Arf1 and Rab GTPases in polarization of the Golgi stack. Traffic *6*, 803–819.

Bannykh, S. I., Rowe, T., and Balch, W. E. (1996). The organization of endoplasmic reticulum export complexes. J. Cell Biol. *135*, 19–35.

Beckers, C. J., Keller, D. S., and Balch, W. E. (1987). Semi-intact cells permeable to macromolecules: use in reconstitution of protein transport from the endoplasmic reticulum to the Golgi complex. Cell *50*, 523–534.

Beckers, C. J., Keller, D. S., and Balch, W. E. (1989). Preparation of semi-intact Chinese hamster ovary cells for reconstitution of endoplasmic reticulum-to-Golgi transport in a cell-free system. Methods Cell Biol. *31*, 91–102.

Beckers, C. J., Plutner, H., Davidson, H. W., and Balch, W. E. (1990). Sequential intermediates in the transport of protein between the endoplasmic reticulum and the Golgi. J. Biol. Chem. *265*, 18298–18310.

Block, M. R., Glick, B. S., Wilcox, C. A., Wieland, F. T., and Rothman, J. E. (1988). Purification of an N-ethylmaleimide-sensitive protein catalyzing vesicular transport. Proc. Natl. Acad. Sci. USA *85*, 7852–7856.

Calero, M., Chen, C. Z., Zhu, W., Winand, N., Havas, K. A., Gilbert, P. M., Burd, C. G., and Collins, R. N. (2003). Dual prenylation is required for Rab protein localization and function. Mol. Biol. Cell *14*, 1852–1867.

Cavalli, V., Vilbois, F., Corti, M., Marcote, M. J., Tamura, K., Karin, M., Arkinstall, S., and Gruenberg, J. (2001). The stress-induced MAP kinase p38 regulates endocytic trafficking via the GDI:Rab5 complex. Mol. Cell *7*, 421–432.

Chandra, S., Gallardo, G., Fernandez-Chacon, R., Schluter, O. M., and Sudhof, T. C. (2005). alpha-Synuclein Cooperates with CSPalpha in Preventing Neurodegeneration. Cell *123*, 383–396.

Cheng, K. W., Lahad, J. P., Gray, J. W., and Mills, G. B. (2005). Emerging role of RAB GTPases in cancer and human disease. Cancer Res. *65*, 2516–2519.

Garrett, M. D., Zahner, J. E., Cheney, C. M., and Novick, P. J. (1994). GDI1 encodes a GDP dissociation inhibitor that plays an essential role in the yeast secretory pathway. EMBO J. *13*, 1718–1728.

Gomes, A. Q., Ali, B. R., Ramalho, J. S., Godfrey, R. F., Barral, D. C., Hume, A. N., and Seabra, M. C. (2003). Membrane targeting of Rab GTPases is influenced by the prenylation motif. Mol. Biol. Cell *14*, 1882–1899.

Gurkan, C., Lapp, H., Alory, C., Su, A. I., Hogenesch, J., and Balch, W. E. (2005). Large-scale profiling of Rab GTPase trafficking networks: the membrome. Mol. Biol. Cell *16*, 3847–3864.

Jez, J. M., Chen, J. C., Rastelli, G., Stroud, R. M., and Santi, D. V. (2003). Crystal structure and molecular modeling of 17-DMAG in complex with human Hsp90. Chem. Biol. *10*, 361–368.

Kamal, A., Thao, L., Sensintaffar, J., Zhang, L., Boehm, M. F., Fritz, L. C., and Burrows, F. J. (2003). A high-affinity conformation of Hsp90 confers tumour selectivity on Hsp90 inhibitors. Nature *425*, 407–410.

Khosravi-Far, R., Lutz, R. J., Cox, A. D., Conroy, L., Bourne, J. R., Sinensky, M., Balch, W. E., Buss, J. E., and Der, C. J. (1991). Isoprenoid modification of rab proteins terminating in CC or CXC motifs. Proc. Natl. Acad. Sci. USA *88*, 6264–6268.

Kimura, Y., Matsumoto, S., and Yahara, I. (1994). Temperature-sensitive mutants of hsp82 of the budding yeast *Saccharomyces cerevisiae*. Mol. Gen. Genet. *242*, 517–527.

Klionsky, D. J. (1998). Nonclassical protein sorting to the yeast vacuole. J. Biol. Chem. *273*, 10807–10810.

Kuge, O., Dascher, C., Orci, L., Rowe, T., Amherdt, M., Plutner, H., Ravazzola, M., Tanigawa, G., Rothman, J. E., and Balch, W. E. (1994). Sar1 promotes vesicle budding from the endoplasmic reticulum but not Golgi compartments. J. Cell Biol. *125*, 51–65.

Lippincott-Schwartz, J., Yuan, L. C., Bonifacino, J. S., and Klausner, R. D. (1989). Rapid redistribution of Golgi proteins into the ER in cells treated with brefeldin A: evidence for membrane cycling from Golgi to ER. Cell *56*, 801–813.

Loo, M. A., Jensen, T. J., Cui, L., Hou, Y., Chang, X. B., and Riordan, J. R. (1998). Perturbation of Hsp90 interaction with nascent CFTR prevents its maturation and accelerates its degradation by the proteasome. EMBO J. *17*, 6879–6887.

Luan, P., Balch, W. E., Emr, S. D., and Burd, C. G. (1999). Molecular dissection of guanine nucleotide dissociation inhibitor function in vivo. Rab-independent binding to membranes and role of Rab recycling factors. J. Biol. Chem. *274*, 14806–14817.

Luan, P., Heine, A., Zeng, K., Moyer, B., Greasely, S. E., Kuhn, P., Balch, W. E., and Wilson, I. A. (2000). A new functional domain of guanine nucleotide dissociation inhibitor (alpha-GDI) involved in Rab recycling. Traffic *1*, 270–281.

Maloney, A., and Workman, P. (2002). HSP90 as a new therapeutic target for cancer therapy: the story unfolds. Expert Opin. Biol. Ther. *2*, 3–24.

Miyata, Y. (2005). Hsp90 inhibitor geldanamycin and its derivatives as novel cancer chemotherapeutic agents. Curr. Pharm. Des. *11*, 1131–1138.

Nathan, D. F., and Lindquist, S. (1995). Mutational analysis of Hsp90 function: interactions with a steroid receptor and a protein kinase. Mol. Cell. Biol. *15*, 3917–3925.

Nishimura, N., Goji, J., Nakamura, H., Orita, S., Takai, Y., and Sano, K. (1995). Cloning of a brain-type isoform of human Rab GDI and its expression in human neuroblastoma cell lines and tumor specimens. Cancer Res. *55*, 5445–5450.

Nishimura, N., Nakamura, H., Takai, Y., and Sano, K. (1994). Molecular cloning and characterization of two rab GDI species from rat brain: brain-specific and ubiquitous types. J. Biol. Chem. *269*, 14191–14198.

Nuoffer, C., Davidson, H. W., Matteson, J., Meinkoth, J., and Balch, W. E. (1994). A GDP-bound of rab1 inhibits protein export from the endoplasmic reticulum and transport between Golgi compartments. J. Cell Biol. *125*, 225–237.

Panaretou, B., Prodromou, C., Roe, S. M., O'Brien, R., Ladbury, J. E., Piper, P. W., and Pearl, L. H. (1998). ATP binding and hydrolysis are essential to the function of the Hsp90 molecular chaperone in vivo. EMBO J. *17*, 4829–4836.

Pearl, L. H. (2005). Hsp90 and Cdc37 –a chaperone cancer conspiracy. Curr. Opin. Genet. Dev. *15*, 55–61.

Pereira-Leal, J. B., Hume, A. N., and Seabra, M. C. (2001). Prenylation of Rab GTPases: molecular mechanisms and involvement in genetic disease. FEBS Lett. *498*, 197–200.

Pereira-Leal, J. B., and Seabra, M. C. (2001). Evolution of the Rab family of small GTP-binding proteins. J. Mol. Biol. *313*, 889–901.

Peter, F., Nuoffer, C., Pind, S. N., and Balch, W. E. (1994). Guanine nucleotide dissociation inhibitor is essential for Rab1 function in budding from the endoplasmic reticulum and transport through the Golgi stack. J. Cell Biol. *126*, 1393–1406.

Pfeffer, S., and Aivazian, D. (2004). Targeting Rab GTPases to distinct membrane compartments. Nat. Rev. Mol. Cell Biol. *5*, 886–896.

Pind, S. N., Nuoffer, C., McCaffery, J. M., Plutner, H., Davidson, H. W., Farquhar, M. G., and Balch, W. E. (1994). Rab1 and Ca2+ are required for the fusion of carrier vesicles mediating endoplasmic reticulum to Golgi transport. J. Cell Biol. *125*, 239–252.

Piper, P. W., Millson, S. H., Mollapour, M., Panaretou, B., Siligardi, G., Pearl, L. H., and Prodromou, C. (2003). Sensitivity to Hsp90-targeting drugs can arise with mutation to the Hsp90 chaperone, cochaperones and plasma membrane ATP binding cassette transporters of yeast. Eur. J. Biochem. *270*, 4689–4695.

Plutner, H., Cox, A. D., Pind, S., Khosravi-Far, R., Bourne, J. R., Schwaninger, R., Der, C. J., and Balch, W. E. (1991). Rab1b regulates vesicular transport between the endoplasmic reticulum and successive Golgi compartments. J. Cell Biol. *115*, 31–43.

Plutner, H., Davidson, H. W., Saraste, J., and Balch, W. E. (1992). Morphological analysis of protein transport from the ER to Golgi membranes in digitonin-permeabilized cells: role of the P58 containing compartment. J. Cell Biol. *119*, 1097–1116.

Pratt, W. B., Galigniana, M. D., Morishima, Y., and Murphy, P. J. (2004). Role of molecular chaperones in steroid receptor action. Essays Biochem. *40*, 41–58.

Pratt, W. B., and Toft, D. O. (1997). Steroid receptor interactions with heat shock protein and immunophilin chaperones. Endocr. Rev. *18*, 306–360.

Pratt, W. B., and Toft, D. O. (2003). Regulation of signaling protein function and trafficking by the hsp90/hsp70-based chaperone machinery. Exp. Biol. Med. (Maywood) *228*, 111–133.

Prodromou, C., and Pearl, L. H. (2003). Structure and functional relationships of Hsp90. Curr. Cancer Drug Targets *3*, 301–323.

Prodromou, C., Roe, S. M., O'Brien, R., Ladbury, J. E., Piper, P. W., and Pearl, L. H. (1997). Identification and structural characterization of the ATP/ADP-binding site in the Hsp90 molecular chaperone. Cell *90*, 65–75.

Pylypenko, O., *et al.* (2006). Structure of doubly prenylated Ypt 1, GDI complex and the mechanism of GDI-mediated Rab recycling. EMBO J. *25*, 13–23.

Rabouille, C., Levine, T. P., Peters, J. M., and Warren, G. (1995). An NSF-like ATPase, p97, and NSF mediate cisternal regrowth from mitotic Golgi fragments. Cell *82*, 905–914.

Rak, A., Pylypenko, O., Durek, T., Watzke, A., Kushnir, S., Brunsveld, L., Waldmann, H., Goody, R. S., and Alexandrov, K. (2003). Structure of Rab GDP-dissociation inhibitor in complex with prenylated YPT1 GTPase. Science *302*, 646–650.

Rink, J., Ghigo, E., Kalaidzidis, Y., and Zerial, M. (2005). Rab conversion as a mechanism of progression from early to late endosomes. Cell *122*, 735–749.

Roe, S. M., Ali, M. M., Meyer, P., Vaughan, C. K., Panaretou, B., Piper, P. W., Prodromou, C., and Pearl, L. H. (2004). The Mechanism of Hsp90 regulation by the protein kinase-specific cochaperone p50(cdc37). Cell *116*, 87–98.

Roe, S. M., Prodromou, C., O'Brien, R., Ladbury, J. E., Piper, P. W., and Pearl, L. H. (1999). Structural basis for inhibition of the Hsp90 molecular chaperone by the antitumor antibiotics radicicol and geldanamycin. J. Med. Chem. *42*, 260–266.

Rowe, T., Aridor, M., McCaffery, J. M., Plutner, H., Nuoffer, C., and Balch, W. E. (1996). COPII vesicles derived from mammalian endoplasmic reticulum microsomes recruit COPI. J. Cell Biol. *135*, 895–911.

Sakisaka, T., Meerlo, T., Matteson, J., Plutner, H., and Balch, W. E. (2002). Rab-alphaGDI activity is regulated by a Hsp90 chaperone complex. EMBO J. *21*, 6125–6135.

Sanford, J. C., Yu, J., Pan, J. Y., and Wessling-Resnick, M. (1995). GDP dissociation inhibitor serves as a cytosolic acceptor for newly synthesized and prenylated Rab5. J. Biol. Chem. *270*, 26904–26909.

Sasaki, T., and Takai, Y. (1995). Purification and properties of bovine Rab-GDP dissociation inhibitor. Methods Enzymol. *257*, 70–79.

Schalk, I., Zeng, K., Wu, S. K., Stura, E. A., Matteson, J., Huang, M., Tandon, A., Wilson, I. A., and Balch, W. E. (1996). Structure and mutational analysis of Rab GDP-dissociation inhibitor. Nature *381*, 42–48.

Schulte, T. W., Akinaga, S., Soga, S., Sullivan, W., Stensgard, B., Toft, D., and Neckers, L. M. (1998). Antibiotic radicicol binds to the N-terminal domain of Hsp90 and shares important biologic activities with geldanamycin. Cell Stress Chaperones *3*, 100–108.

Sherman, F. (1986). Translation, post-translational processing, and mitochondrial translocation of yeast iso-1-cytochrome c. Basic Life Sci. *40*, 533–544.

Shisheva, A., Sudhof, T. C., and Czech, M. P. (1994). Cloning, characterization, and expression of a novel GDP dissociation inhibitor isoform from skeletal muscle. Mol. Cell. Biol. *14*, 3459–3468.

Soldati, T., Riederer, M. A., and Pfeffer, S. R. (1993). Rab GDI: a solubilizing and recycling factor for rab9 protein. Mol. Biol. Cell *4*, 425–434.

Sudhof, T. C. (2004). The synaptic vesicle cycle. Annu. Rev. Neurosci. *27*, 509–547.

Tisdale, E. J., Bourne, J. R., Khosravi-Far, R., Der, C. J., and Balch, W. E. (1992). GTP-binding mutants of rab1 and rab2 are potent inhibitors of vesicular transport from the endoplasmic reticulum to the Golgi complex. J. Cell Biol. *119*, 749–761.

Ullrich, O., Stenmark, H., Alexandrov, K., Huber, L. A., Kaibuchi, K., Sasaki, T., Takai, Y., and Zerial, M. (1993). Rab GDP dissociation inhibitor as a general regulator for the membrane association of rab proteins. J. Biol. Chem. *268*, 18143–18150.

Vega, V. L., and De Maio, A. (2003). Geldanamycin treatment ameliorates the response to LPS in murine macrophages by decreasing CD14 surface expression. Mol. Biol. Cell *14*, 764–773.

Whiteheart, S. W., Rossnagel, K., Buhrow, S. A., Brunner, M., Jaenicke, R., and Rothman, J. E. (1994). N-Ethylmaleimide-sensitive fusion protein: a trimeric ATPase whose hydrolysis of ATP is required for membrane fusion. J. Cell Biol. *126*, 945–954.

Wilson, B. S., Nuoffer, C., Meinkoth, J. L., McCaffery, M., Feramisco, J. R., Balch, W. E., and Farquhar, M. G. (1994). A Rab1 mutant affecting guanine nucleotide exchange promotes disassembly of the Golgi apparatus. J. Cell Biol. *125*, 557–571.

Zhao, R., *et al.* (2005). Navigating the chaperone network: an integrative map of physical and genetic interactions mediated by the hsp90 chaperone. Cell *120*, 715–727.